

## Ni/SiC: a stable and active catalyst for catalytic partial oxidation of methane

Pascaline Leroi<sup>a</sup>, Behrang Madani<sup>a</sup>, Cuong Pham-Huu<sup>a,\*</sup>, Marc-Jacques Ledoux<sup>a</sup>, Sabine Savin-Poncet<sup>b</sup>, Jacques Louis Bousquet<sup>b</sup>

<sup>a</sup> *Laboratoire des Matériaux, Surfaces et Procédés pour la Catalyse, UMR 7515 du CNRS, ECPM, ULP, ELCASS (European Laboratory for Catalysis and Surface Science), 25 Rue Becquerel, 67037 Strasbourg Cedex 2, France*

<sup>b</sup> *Total, Direction Stratégie Croissance Recherche, Valorisation des Gaz Naturels, 64018 Pau Cedex, France*

### Abstract

A nickel catalyst supported on medium surface area  $\beta$ -SiC was successfully used in the partial oxidation of methane into synthesis gas. The high thermal conductivity of the SiC support prevented the formation of hot spots on the catalyst surface at the start of the reaction in contrast to what is observed on a traditional alumina-based insulated catalyst. Carbon nanofilament growth did not occur on the SiC-based catalyst. The combination of hot spot and carbon nanofilament formation led to the complete destruction of the body shape of the alumina-based catalyst after reaction whereas the SiC-based catalyst still retained its macroscopic shape.

© 2004 Elsevier B.V. All rights reserved.

*Keywords:* Nanofilament; SiC; Nickel

### 1. Introduction

Synthesis gas, a mixture of  $H_2$  and CO, is an important feed-stock for several chemical processes used in the production of methanol and synthetic fuels or other intermediates through a Fischer–Tropsch synthesis [1]. The hydrogen can be also separated for subsequent use in the ammonia plant or to generate electrical energy via fuel cells [2]. Synthesis gas is nowadays industrially produced via steam reforming of methane which is a highly endothermic reaction ( $CH_4 + H_2O \rightarrow CO + 3H_2$ ,  $\Delta H = +225.4 \text{ kJ mol}^{-1}$ ). However, the  $H_2/CO$  ratio produced from the steam reforming process is too high for the methanol and the Fischer–Tropsch syntheses and thus, for the last two decades research has been oriented towards synthesis gas production via direct catalytic partial oxidation ( $CH_4 + (1/2)O_2 \rightarrow CO + 2H_2$ ,  $\Delta H = -38 \text{ kJ mol}^{-1}$ ) and the  $CO_2$  reforming of methane ( $CH_4 + CO_2 \rightarrow 2CO + 2H_2$ ,  $\Delta H = +247 \text{ kJ mol}^{-1}$ ). The main disadvantage of these processes is the high coke formation which constitutes a serious problem in their industrial application [3–6]. Coke, essentially in

the nanofilament form, may cause severe deactivation of the catalyst surface, blocking of the catalyst pores and sometimes, physical disintegration of the catalyst support body which can induce a pressure drop along the catalyst bed, in some cases, inducing damage to the reactor itself [7,8]. Coke formation is also favoured in the catalytic partial oxidation (CatPOx) process by hot spot formation on the catalyst surface due to the inability of the traditional insulator supports, i.e. alumina and silica, to evacuate the heat formed [9–11]. It is of interest to find a new type of support having the same advantages as those of the alumina or silica-based supports but with a high thermal conductivity and mechanical strength in order to avoid the problems of hot spot and coke formation and also to maintain the catalyst body integrity.

Silicon carbide (cubic  $\beta$ -SiC) exhibits a high thermal conductivity, a high resistance towards oxidation, a high mechanical strength, a low specific weight, and chemical inertness, all of which make it a good candidate for use as catalyst support material in place of the traditional insulator supports in several highly endothermic or exothermic reactions or in aggressive reaction media, i.e. strong acidic or basic solution [12].

The aim of the present article is to report catalytic behaviour in the catalytic partial oxidation of methane over a Ni/SiC catalyst with high thermal conductivity

\* Corresponding author. Tel.: +33-3-90-24-26-75; fax: +33-3-90-24-26-74.

E-mail address: [cuong.lcmc@ecpm.u-strasbg.fr](mailto:cuong.lcmc@ecpm.u-strasbg.fr) (C. Pham-Huu).

and mechanical strength [13]. The catalyst, before and after reaction, was characterised using several different techniques, i.e. transmission electron microscopy (TEM), temperature-programmed oxidation (TPO) coupled with mass spectrometry detection and specific surface area measurements, to obtain detailed information about the nature and the amount of the carbon species formed on the catalyst during the test. The catalytic performance obtained on the Ni/SiC catalyst was also compared with that of the traditional Ni/ $\gamma$ -Al<sub>2</sub>O<sub>3</sub> catalyst tested under similar reaction conditions.

## 2. Experimental

### 2.1. Supports and catalysts

Silicon carbide in an extrudate form (2 mm × 6 mm) with a medium BET surface area of 25 m<sup>2</sup> g<sup>-1</sup> was supplied by Pechiney [14]. The support contained both mesopores (40 nm) and macropores (micrometer size measured by mercury intrusion) with a complete absence of micropores. A detailed description of the synthesis method has already been reported elsewhere [11,15]. A commercial  $\gamma$ -alumina support in an extrudate shape (2 mm × 6 mm) with a surface area of 220 m<sup>2</sup> g<sup>-1</sup> and mesoporous contribution was used for comparison. The nickel was deposited on the two supports via wetness impregnation using an aqueous solution of nickel nitrate. After impregnation the solid was calcined in air at 350 °C for 2 h in order to decompose the nitrate into its corresponding oxide. The theoretical nickel loading was set to be 4.7 wt. %.

### 2.2. Catalytic test

Catalytic tests were carried out in a fixed tubular Hasteloy reactor (1200 mm length, 6 mm inner diameter). The reactor system was purged with argon at atmospheric pressure and room temperature for 30 min before admitting the reactant mixture. Gas flow rates were controlled by a mass flow controller (Brooks TR 5848). The catalytic partial oxidation reaction was carried out with a mixture of CH<sub>4</sub>:O<sub>2</sub> of 2.5 and a total flow rate of 100 ml min<sup>-1</sup> (space velocity of 1200 h<sup>-1</sup>) corresponding to a contact time of 3 s, under a total pressure of 0.5 MPa and a reaction temperature of 900 °C. The high CH<sub>4</sub>-to-O<sub>2</sub> ratio was chosen in order to enhance the deactivation rate by coke formation and to work as close as possible under the severe reaction conditions. Analyses of reactant/product mixtures were achieved by a model Varian-3800 gas chromatograph with an on-line thermal conductivity and flame ionisation detectors.

### 2.3. Characterisation techniques

The powder X-ray diffraction (XRD) was carried out using a Siemens D-5000 diffractometer working with a

Cu K $\alpha$  non-monochromatic radiation in a  $\theta/2\theta$  mode. The diffraction lines were compared with those of the JCPDS data bank (Joint Committee Powder Diffraction Standard). TEM was carried out on a Topcon 002B UHR microscope worked under 200 kV accelerated voltage and which allowed a point-to-point resolution of 0.17 nm. The sample was dispersed in ethanol in an ultrasonic bath and then was deposited dropwise on a holey carbon-coated copper grid for examination. The specific surface area was carried out on a Coulter SA-3100 sorptometer using N<sub>2</sub> as adsorbent at the liquid nitrogen temperature (-196 °C). Before measurement the sample was outgassed at 200 °C for 2 h in order to desorb impurities and moisture on its surface. The amount of carbon deposited on the catalyst was investigated by means of the temperature-programmed oxidation technique coupled with mass spectrometry detection (CO<sub>2</sub>,  $m/z = 44$ ). The sample was heated in flowing O<sub>2</sub> (10 vol.%) in helium with a flow rate of 20 ml min<sup>-1</sup> and the heating rate was set at 10 °C min<sup>-1</sup>.

## 3. Results and discussion

### 3.1. Catalytic activity

The catalytic activity and the H<sub>2</sub>/CO ratio of the Ni/SiC catalyst under 0.5 MPa are presented in Fig. 1A. The experimental conversion was identical to that predicted by the thermodynamic calculations with a CH<sub>4</sub>:O<sub>2</sub> ratio of 2.5 and shows that no catalyst temperature runaway occurred during the test, in good agreement with the high thermal conductivity of the SiC support [16]. The catalytic conversion remained unchanged up to 100 h on stream indicating the complete absence of deactivation under the reaction conditions. It is well known that during this type of reaction a large amount of carbon is formed on the catalyst surface inducing deactivation [17–19]. It seems from the observed results that the carbon deposited on the SiC-based catalyst was not enough to encapsulate the active sites. More detailed characterisation results on the carbon formed on the SiC-based catalyst are presented below. The catalyst surface area remains unchanged after reaction at about 25 m<sup>2</sup> g<sup>-1</sup> which highlighted the thermal resistance of the SiC-based catalyst.

The catalytic activity of the Ni/ $\gamma$ -Al<sub>2</sub>O<sub>3</sub> catalyst is presented in Fig. 1B under the same reaction conditions. On the alumina-based catalyst, the conversion was significantly higher at the beginning of the test, i.e. about 15% over that predicted by thermodynamic calculations, which was attributed to hot spot formation on the catalyst surface due to the exothermic character of the reaction, inducing temperature runaway due to the insulation properties of the support. The conversion slowly decreased to the thermodynamic level after about 30 h of test and remained stable for the rest of the test.

The low thermal conductivity of the alumina support was not able to rapidly evacuate the heat formed during the

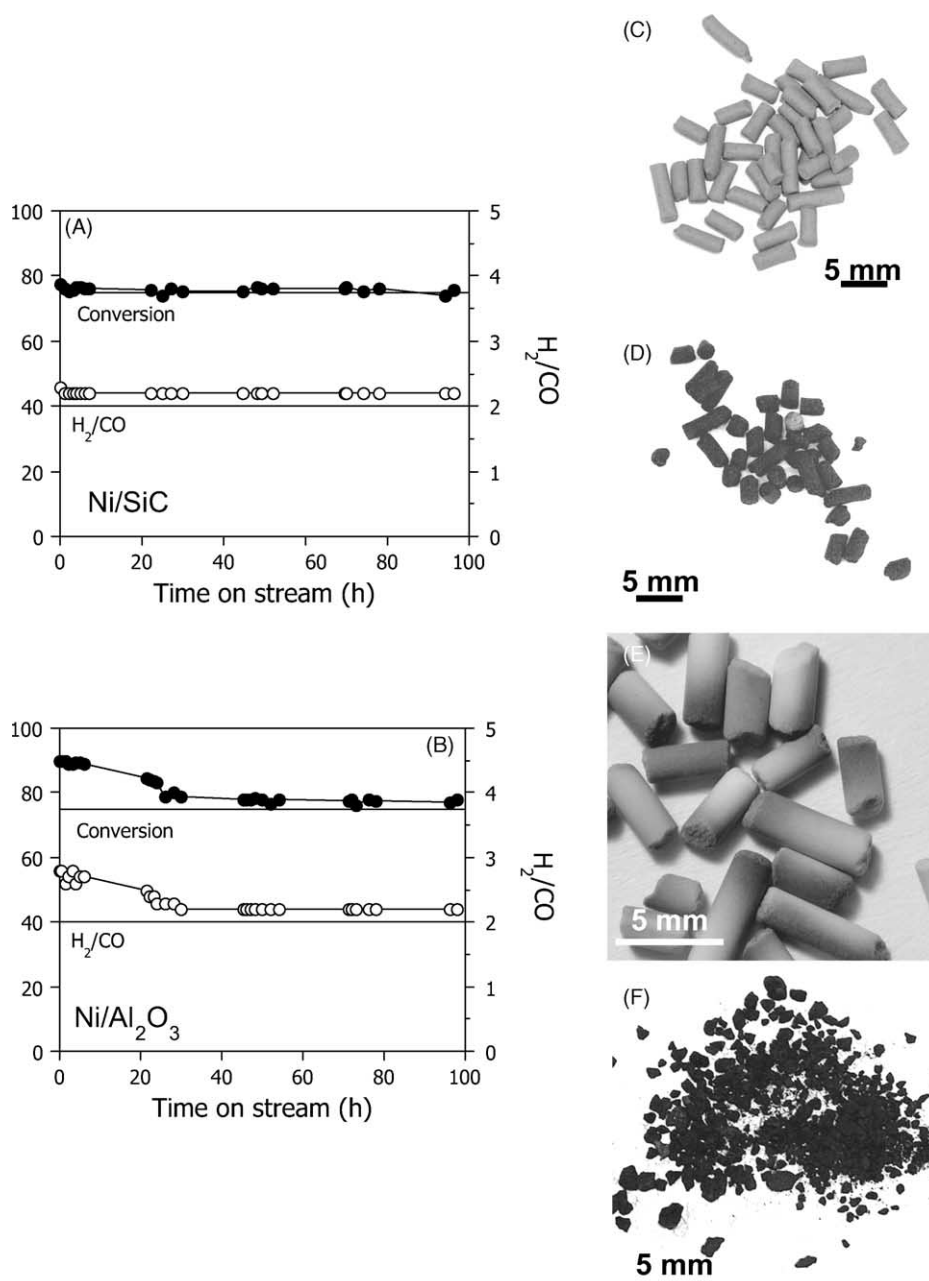


Fig. 1. Methane reformation activity of the (A) SiC-based and (B) alumina-based catalysts; (C) and (D) optical images of the SiC-based catalyst before and after reaction; (E) and (F) optical images of the alumina-based catalyst before and after reaction.

reaction resulting in a temperature runaway. As a function of time on stream, the carbon deposit on the catalyst surface slowly increased the thermal conductivity of the catalyst surface which resulted in a decrease in the conversion to the thermodynamic level. The formation of hot spots during the partial oxidation of methane on insulator supports has already been reported by several authors in the literature [20–22]. The hot spot formation also significantly modified the H<sub>2</sub>:CO molar ratio which amounted to about 2.8 instead of 2, i.e. excess hydrogen production by methane decomposition. The ratio slightly decreased with time on stream to reach the theoretical value of 2.

The specific surface area of the alumina-based catalyst also significantly decreased after the reaction, i.e. 64 m<sup>2</sup> g<sup>-1</sup> instead of 230 m<sup>2</sup> g<sup>-1</sup>. Such result was attributed to the support phase transition from the high surface area  $\gamma$ -Al<sub>2</sub>O<sub>3</sub> to the low surface area  $\alpha$ -Al<sub>2</sub>O<sub>3</sub> according to the XRD pattern (not shown).

### 3.2. Macroscopic morphology conservation

The optical image shows that the SiC-based catalyst exhibited no macroscopic morphology change after the catalytic test (Fig. 1C and D) whereas the alumina-based

catalyst was completely destroyed, with only small particles and fine powder remaining (Fig. 1E and F).

The catalyst body destruction observed on the alumina-based catalyst is extremely detrimental for its use in fixed-bed processes as it generates pressure drop and loss of the active phase. The spent catalysts were also darker indicating the presence of a carbonaceous residue on their surfaces in agreement with the hypothesis advanced above and with the results reported in the literature [23]. X-ray powder diffraction analysis has shown that no trace of NiO has been observed confirming that the deactivation observed on the alumina-based catalyst was mainly due to coke formation and not to the oxidation of the Ni active site back to an inactive NiO species as reported by Yan et al. [24] over Ni/TiO<sub>2</sub> catalyst. The hot spot formation at the start of the test also induces the formation of low surface area alumina phases, i.e.  $\delta$ -Al<sub>2</sub>O<sub>3</sub> and  $\theta$ -Al<sub>2</sub>O<sub>3</sub>, from the high surface area  $\gamma$ -Al<sub>2</sub>O<sub>3</sub> according to the XRD results (not shown).

### 3.3. Microstructural and oxidative behaviour of the carbon species

On the SiC-based catalyst, the carbon was present in either turbostratic or amorphous structures (Fig. 2A). A high resolution TEM image (inset of Fig. 2A) shows that the turbostratic carbon has a short range order with only a few graphene planes. In some area of the catalyst some carbon nanofibres was also observed. However, statistical measurement by TEM have show that these carbon nanofibres only amounted to few percents of the total amount of carbon formed on the catalyst.

On the other hand, the carbon species formed on the alumina-based catalyst were essentially nanofilamentous in nature with an average diameter of about 50 nm and length up to micrometer range (Fig. 2B) in agreement with the published results for such catalytic systems [25–27]. A high resolution TEM image (inset of Fig. 2B) shows that the nanofilaments were highly graphitised in nature with exposed prismatic planes which is typical for carbon nanostructure growth from a nickel catalyst [28,29]. Apparently, the nickel phase supported on the SiC surface was not able to form carbon nanofilaments unlike the nickel supported on the alumina carrier. This phenomenon could be attributed to the different interactions between the nickel and the SiC surface which led to the formation of peculiar exposed nickel faces which were not able to grow carbon nanofilaments. It is well documented in the literature that only certain faces of nickel are active for carbon nanostructure formation while others are not, resulting in the formation of a loosely ordered carbon structure [9,13]. One cannot also exclude the influence of the nickel particle size on the carbon nanofibres formation on the tested catalysts. Work is underway to confirm such hypothesis using nickel metal with different exposed faces and average particle size.

The formation of different carbon structures from the nickel surface observed above could be attributed to the

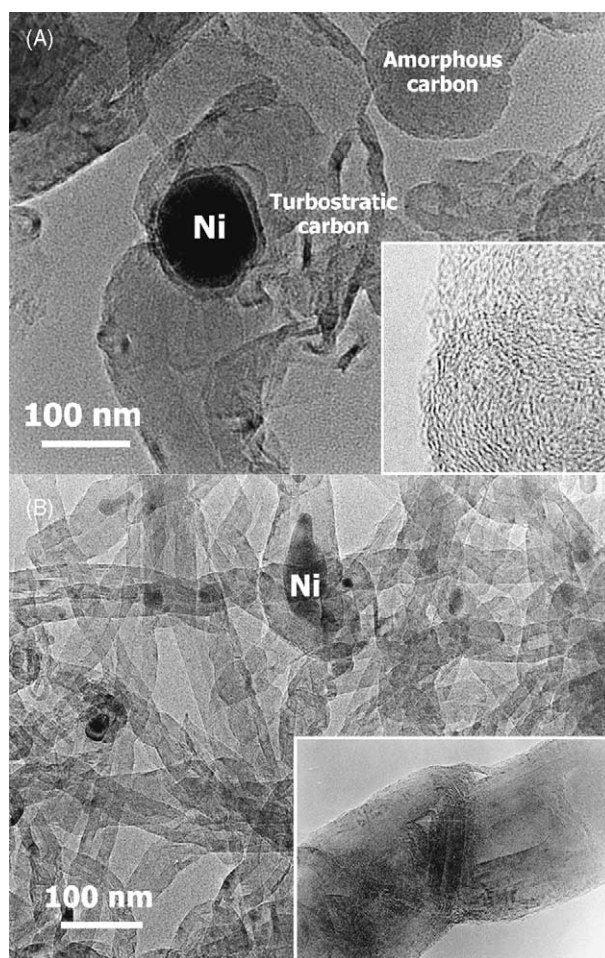


Fig. 2. TEM micrographs of the carbonaceous formed on the (A) SiC-based and (B) alumina-based catalysts. High-resolution TEM micrographs of the carbon species are presented in the inset.

existence of different metal–support interactions which modified the exposed faces of the metal leading to different carbon nucleation and growth. On the alumina-based catalyst, the strong interactions between the nickel particles and the alumina surface could have altered the electronic properties of the nickel which could have favoured the active nickel faces for hydrocarbon decomposition and carbon filament growth. The low interactions between the nickel and the SiC surface could have induced the change on the nickel exposed faces and thus, significantly altered the rate of carbon nanofilament formation. The formation of carbon filaments inside the alumina matrix explains why the support body broke after the catalytic tests since they have extremely high mechanical strength and aspect ratio. The distance between the graphene planes was about 0.33–0.34 nm which is very similar to that of graphite (0.335 nm). These kinds of carbon deposits have already been reported by several groups [30,31]. It should be noted that TEM images clearly evidence the complete absence of nickel particles on the carbon nanofibre tip indicating that the growth mode is a base growth mechanism where the

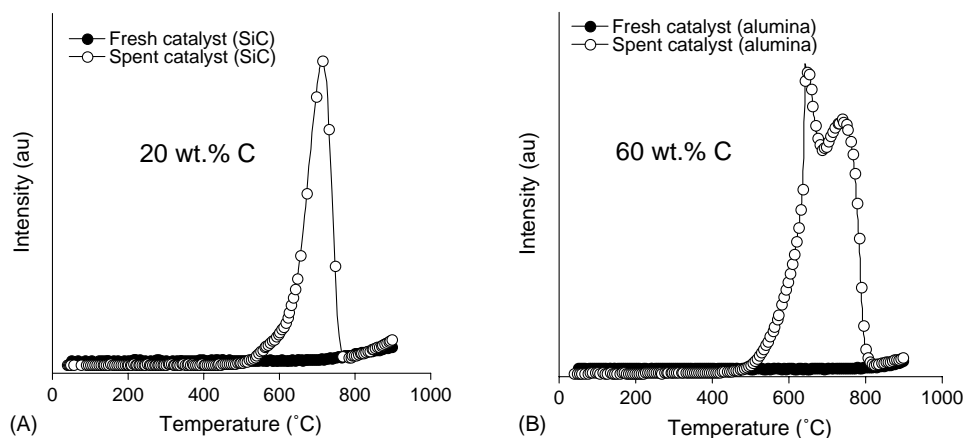


Fig. 3. TPO spectra of the carbonaceous formed on the (A) SiC-based and (B) alumina-based catalysts showing the difference in the carbon nature. Analysis conditions—heating rate:  $10^{\circ}\text{C min}^{-1}$  from room temperature to  $900^{\circ}\text{C}$ ,  $\text{O}_2$  (20 vol.%) in helium with a total flow rate of  $20\text{ ml min}^{-1}$ . The TPO surface peak between the two catalysts was not normalised.

catalyst particle remains anchored on the support surface [26].

Temperature-programmed oxidation carried out on the spent catalysts also revealed the formation of a higher amount of carbon on the alumina catalyst compared to the SiC-based catalyst, i.e. 60 wt.% instead of 20 wt.% (Fig. 3). The higher amount of carbon formed on the alumina-based catalyst was attributed to methane decomposition due to the formation of hot spots on the catalyst surface and also to carbon filament formation due to the secondary reaction between the  $\text{CO:H}_2$  products and the nickel sites at the beginning of the reaction. On the SiC-based catalyst the rapid heat evacuation out of the catalyst bed probably played an important role in the low carbon content observed. It is also worth noting that on the SiC-based catalyst the high temperature oxidation peak was not observed as for the alumina-based catalyst which represents roughly 60% of the total amount of carbon deposit. This phenomenon could be attributed to the fact that on the SiC-based catalyst the carbon species formed were less graphitic than that observed on the alumina-based catalyst owing to the high thermal conductivity of the SiC support which allows the lowering of the catalyst surface temperature.

#### 4. Conclusion

From the results observed Ni/SiC seems to be the most promising catalyst for performing the catalytic partial oxidation of methane at medium reaction pressure. The high thermal conductivity of the support means that the temperature runaway on the catalyst surface can be significantly reduced while the high mechanical strength allows the complete conservation of the catalyst body after reaction. The SiC-based catalyst also exhibits an extremely high stability as a function of time on stream which is probably due to

the low carbon deposits. Under the same reaction conditions, the alumina-based catalyst was completely destroyed leaving only a fine powder.

#### Acknowledgements

The authors would like to thank Mrs. G. Ehret (GSI, Institut de Physique et Chimie des Matériaux de Strasbourg, UMR 7504 CNRS) for performing TEM experiments.

#### References

- [1] M. Stelmachowski, L. Nowicki, *Appl. Energy* 74 (2003) 85.
- [2] Z.W. Liu, K.W. Jun, H.S. Roh, S.E. Park, *J. Power Sour.* 111 (2002) 283.
- [3] B.S. Liu, C.T. Au, *Appl. Catal. A* 224 (2003) 181.
- [4] Z. Zhang, X.E. Verykios, S.M. McDonald, S. Affrossman, *J. Chem. Phys.* 100 (1996) 744.
- [5] Y.H. Hu, E. Ruckenstein, *J. Catal.* 184 (1999) 298.
- [6] H.Y. Wang, E. Ruckenstein, *Appl. Catal. A* 204 (2000) 143.
- [7] C.H. Bartholomew, *Catal. Rev.-Sci. Eng.* 24 (1982) 67.
- [8] J.R. Rostrup-Nielsen, *Catal. Today* 63 (2000) 159.
- [9] H.Y. Wang, E. Ruckenstein, *Catal. Lett.* 59 (1999) 121.
- [10] Y. Ji, W. Li, H. Xu, Y. Chen, *Appl. Catal. A* 213 (2001) 25.
- [11] S. Liu, G. Xiong, H. Dong, W. Yang, *Appl. Catal. A* 202 (2000) 141.
- [12] M.J. Ledoux, C. Pham-Huu, *CATTECH* 5 (2001) 226.
- [13] C. Pham-Huu, P. Leroi, M.J. Ledoux, S. Savin-Poncet, J.L. Bousquet, PCT Application No. FR02-02093 (2002).
- [14] G. Baluais, B. Ollivier, PCT WO-98/30328 (1998).
- [15] M.J. Ledoux, C. Pham-Huu, *Catal. Today* 15 (1992) 263.
- [16] M.J. Ledoux, C. Crouzet, C. Pham-Huu, V. Turines, K. Kourtakis, P.L. Mills, J.J. Lerou, *J. Catal.* 203 (2001) 495.
- [17] P. Chen, H.B. Zhang, G.D. Lin, K.R. Tsai, *Appl. Catal. A* 166 (1998) 343.
- [18] A.M. de Groote, G.F. Froment, *Catal. Today* 37 (1997) 309.
- [19] H. Moriaka, Y. Shimizu, M. Sukenobu, K. Ito, E. Tanabe, T. Shishido, K. Takehira, *Appl. Catal. A* 215 (2001) 11.
- [20] Y.F. Chang, H. Heinemann, *Catal. Lett.* 21 (1993) 215.

- [21] D. Dissanayake, M.P. Rosynek, J.H. Lunsford, *J. Phys. Chem.* 97 (1993) 3644.
- [22] W.J.M. Vermeiren, E. Blomsma, P.A. Jacobs, *Catal. Today* 13 (1992) 427.
- [23] J.R. Rostrup-Nielsen, *Catal. Today* 63 (2000) 159.
- [24] Q.G. Yan, W.Z. Weng, H.L. Wan, H. Toghiani, R.K. Toghiani, C.U. Pittman Jr., *Appl. Catal. A* 239 (2003) 43.
- [25] K.P. de Jong, J.W. Geus, *Catal. Rev.-Sci. Eng.* 42 (2000) 481.
- [26] C. Laurent, E. Flahaut, A. Peigney, A. Rousset, *New J. Chem.* (1998) 1229.
- [27] M.A. Ermakova, D.Y. Ermakov, A.L. Chuvilin, G.G. Kuvshinov, *J. Catal.* 201 (2001) 183.
- [28] C. Pham-Huu, N. Keller, V.V. Roddatis, G. Mestl, R. Schlögl, M.J. Ledoux, *Phys. Chem.-Chem. Phys.* 4 (2002) 514.
- [29] R. Vieira, C. Pham-Huu, N. Keller, M.J. Ledoux, *Chem. Commun.* (2002) 954.
- [30] Y. Zhang, G. Xiong, S. Sheng, W. Yang, *Catal. Today* 63 (2000) 517.
- [31] J.B. Claridge, M.L.H. Green, S.C. Tsang, A.P.E. York, A.T. Ashcroft, P.D. Battle, *Catal. Lett.* 22 (1993) 299.